



In Vitro Effects of Lead on Gene Expression in Neural Stem Cells and Associations between Upregulated Genes and Cognitive Scores in Children

Peter J. Wagner, Hae-Ryung Park, Zhaoxi Wang, Rory Kirchner, Yongyue Wei, Li Su, Kirstie Stanfield, Tomas R. Guilarte, Robert O. Wright, David C. Christiani, and Quan Lu

<http://dx.doi.org/10.1289/EHP265>

Received: 1 December 2015

Revised: 26 July 2016

Accepted: 26 July 2016

Published: 26 August 2016

Note to readers with disabilities: *EHP* will provide a [508-conformant](#) version of this article upon final publication. If you require a 508-conformant version before then, please contact ehp508@niehs.nih.gov. Our staff will work with you to assess and meet your accessibility needs within 3 working days.



National Institute of
Environmental Health Sciences

***In Vitro* Effects of Lead on Gene Expression in Neural Stem Cells and Associations between Upregulated Genes and Cognitive Scores in Children**

Peter J. Wagner,^{1,2} Hae-Ryung Park,^{1,2} Zhaoxi Wang,¹ Rory Kirchner,³ Yongyue Wei,¹ Li Su,¹
Kirstie Stanfield,⁴ Tomas R. Guilarte,⁴ Robert O. Wright,⁵ David C. Christiani,² and Quan Lu^{1,2,6}

¹Department of Environmental Health, ²Program in Molecular and Integrative Physiological Sciences, ³Department of Biostatistics, ⁶Department of Genetics and Complex Diseases, Harvard T.H. Chan School of Public Health, Boston, Massachusetts, USA; ⁴Department of Environmental Health Sciences, Columbia University Mailman School of Public Health, New York City, New York, USA; ⁵Department of Preventative Medicine, Mount Sinai School of Medicine, New York City, New York, USA

Address correspondence to Quan Lu, Harvard School of Public Health, 665 Huntington Avenue, Boston, MA 02215, USA. Telephone: 617-4327145. E-mail: glu@hsph.harvard.edu

Running title: A novel NRF2 target SPP1 and Pb neurotoxicity

Acknowledgements: This study was funded by the Harvard Superfund Research Program (P42ES16454), NIEHS R01 grants (ES015533, ES022230, and ES006189), and the Harvard NIEHS Center grant (P30ES000002). PJW was supported by the Joseph D. Brain and Jere Meade Fellowships as well as the NIH Training grant on Interdisciplinary Pulmonary Sciences (5T32HL007118).

Competing financial interests: All authors declare that they do not have financial or non-financial competing interests.

Abstract

Background: Lead (Pb) adversely affects neurodevelopment in children. Neural stem cells (NSCs) play an essential role in shaping the developing brain, yet little is known about how Pb perturbs NSC functions and whether such perturbation contributes to impaired neurodevelopment.

Objectives: We aimed to identify Pb-induced transcriptomic changes in NSCs and to link these changes to neurodevelopmental outcomes in children who were exposed to Pb.

Methods: We performed RNA-seq-based transcriptomic profiling in human NSCs treated with 1 μ M Pb. We used qRT-PCR, Western blotting, ELISA, and ChIP (Chromatin immunoprecipitation) to characterize Pb-induced gene upregulation. Through interrogation of a genome-wide association study, we examined the association of gene variants with neurodevelopment outcomes in the ELEMENT birth cohort.

Results: We identified 19 genes with significantly altered expression, including many known targets of NRF2—the master transcriptional factor for the oxidative stress response. Pb induced the expression of *SPP1* (secreted phosphoprotein 1), which has known neuroprotective effects. We demonstrated that *SPP1* is a novel direct NRF2 target gene. A SNP (rs12641001) in the regulatory region of *SPP1* exhibits a statistically significant association ($p=0.005$) with the Cognitive Development Index (CDI).

Conclusion: Our findings revealed that Pb induces an NRF2-dependent transcriptional response in neural stem cells and identified SPP1 upregulation as a potential novel mechanism linking Pb exposure with neural stem cell function and neurodevelopment in children.

Introduction

As a pervasive environmental toxicant, lead (Pb) particularly impairs the functions of the neural system (Bellinger 2013; Toscano and Guilarte 2005). While policy limiting the use of Pb has been successful in reducing blood Pb levels in US children (Jones et al. 2009), Pb levels in the environment remain high in many countries where Pb has not – or has only recently – been phased out from gasoline, paint and other applications. In the US over half a million 1-5 year-old children still have blood Pb levels exceeding 10 µg/dL, twice the current threshold of concern defined by the Center of Disease Control (Jones et al. 2009). Pb exposure in children has been consistently linked to impaired neurological development and cognitive dysfunction as well as persistent antisocial and delinquent behavior (Bellinger et al. 1987; Canfield et al. 2003; Needleman et al. 1996). Recent incidences of Pb contamination in drinking water in several US cities highlight the continued threat of Pb to public health, especially to children's health (Bellinger 2016; Levin 2016).

Pb neurotoxicity is determined by intricate interplays between the metal and target neural cells, and there is overwhelming evidence documenting the detrimental effects of Pb in neurons. Seminal studies by Alkondon et al. (Alkondon et al. 1990) and Guilarte et al. (Guilarte and Miceli 1992) showed that Pb potently inhibits the NMDA receptor, which plays an essential role in brain development, synaptic plasticity and learning & memory. Pb also inhibits the vesicular release of BDNF (brain-derived neurotrophic factor) and subsequent TrkB (tropomyosin-related kinase B) activation in the presynaptic neuron (Neal et al. 2010; Neal et al. 2011; Stansfield et al. 2012).

Pb exposure at the early stages of brain development has long-lasting effects on neurocognitive function. Prenatal Pb exposure has been associated with lower mental

development index scores (Bellinger et al. 1987; Hu et al. 2006), and increased risk of schizophrenia later in life (Opler et al. 2004; Opler et al. 2008). In predictive models of mental developmental index (MDI), first trimester Pb exposure assessed in maternal blood was the most pronounced and statistically significant predictor when compared to exposure at any later stages (Hu et al. 2006). The particular susceptibility of early brain development to Pb exposure may be explained, in part, by the metal's effects on neural stem cells (NSCs). As the progenitor cells of all cell types of the central nervous system, NSCs play an essential role in shaping the developing brain and could very well be affected by Pb exposure. Indeed, several studies have shown that Pb slows proliferation of NSCs both *in vitro* (Breier et al. 2008; Huang and Schneider 2004) and *in vivo* (Breier et al. 2008; Gilbert et al. 2005; Schneider et al. 2005; Verina et al. 2007), and alters gene expression to affect neuronal differentiation of mouse (Sanchez-Martin et al. 2013) and human stem cells (Senut et al. 2014).

Despite the known detrimental effects of Pb in NSCs, the underlying molecular mechanisms remain poorly understood, and moreover, whether such effects contribute to the impaired neurodevelopment in children is not known. In this study, we performed global transcriptional profiling to assess the impact of Pb exposure on NSCs. We characterized one of the gene hits, *SPPI* (also known as osteopontin), as a novel NRF2 target and determined whether genetic polymorphisms within the gene are associated with neurological outcomes in children in an epidemiological cohort. We integrated global gene expression profiling with genetic epidemiology and identified a potential mechanistic link between Pb-induced gene expression in NSCs and neurodevelopment in children..

Materials and Methods

NSC culturing, Pb treatment and siRNA transfection

NSCs derived from NIH-approved H9 (WA09) human embryonic stem cells were purchased from Life Technologies and cultured according to supplier's protocol. An aqueous solution of 1 mM Pb acetate trihydrate (cat #316512, Sigma Aldrich) stock was used in all experiments. Transfection of siRNAs was performed with Dharmafect 1 (ThermoFisher) following manufacturer's protocol. All siRNAs were obtained from Sigma: non-targeting control (SIC001), si-NRF2-1 (SASI_Hs01_00182393), si-NRF2-2 (SASI_Hs02_00341015) and si-KEAP1 (SASI_Hs01_00080908). All experiments were performed in passage 3 cells.

Cell viability and growth assays

For the MTT (3-[4,5-dimethylthiazol-2-yl]-2,5-diphenyl tetrazolium bromide) assay, cells were seeded 24 hours prior to exposure at 1×10^4 per well of a 96 well plate. Exposure to 0, 0.5, 1, 2, 5 and 10 μ M Pb was performed in 8 replicate wells. The assay was performed according to the MTT manufacturer's protocol (Sigma Aldrich). Briefly, 0.05 mg of MTT was added to each well for 3 hours. Formazan crystals are solubilized in 10% Triton X-100 plus and 0.1 N HCl in anhydrous isopropanol after repeated pipetting. Absorbance was read at 570 nm, and background at 690 nm removed. Mean absorbance, which is correlated with cell number, is reported along with the standard error of the mean of 8 replicate samples. For growth assay, hNSCs were seeded in 24 well plates at 5×10^4 per well and treated with control vehicle PBS or human recombinant SPP1 protein (Eton Bioscience) at 50 or 250 ng/ml. The next day, hNSCs were exposed to 2 μ M Pb for 3 days. Cell counting was done by hemocytometer with Trypan blue staining to exclude dead cells. Six replicates were done for each condition.

RNA-seq library preparation and sequencing

Poly-adenylated RNA species were isolated from 1 µg of total RNA and converted to a cDNA library for RNA sequencing using the TruSeq RNA v2 kit (Illumina). Sample preparation involves isolating poly-adenylated RNA, RNA fragmentation, cDNA synthesis, ligation of adapters, PCR amplification using DNA barcodes, and library validation and quantification. Four samples were multiplexed into a single lane of the Illumina HiSeq 2000 for paired-end reads of 100 bp. Sequencing was performed at the Bauer Core Illumina Sequencing Facility (FAS Center for Systems Biology, Cambridge MA).

Processing and analysis of RNA-seq data

Low quality reads (<25 phred), adaptors and poly-A tails were trimmed with Cutadapt (Martin 2011). Read pairs with one or more reads shorter than 20 base pairs were removed. Quality of reads was assessed using FASTQC (Babraham Bioinformatics). Reads were aligned to human genome build 19 using Tophat2 (Trapnell et al. 2009) and compiled into count tables using HTseq-count (Gibbs 2003). Counts were normalized in edgeR (Robinson and Oshlack 2010). Differential expression was determined by a generalized linear model. Differentially regulated transcripts were identified following a Benjamini-Hochberg multiple testing correction ($q < 0.05$) that had a greater than ± 0.2 fold change and a minimum counts per million mapped of one.

qRT-PCR

RNA was reverse transcribed using SuperScript III reverse transcriptase and oligo-dT (Life Technologies). The resulting cDNA was amplified using 2x SYBR mix (Qiagen) and 3 mM of each primer in a StepOne Plus Thermocycler (Applied Biosystems) in Quantitative Reverse Transcriptase Polymerase Chain Reaction (qRT-PCR). Melt curves were checked for single-length amplification products. Fold changes were calculated using the $2^{-\Delta\Delta C_t}$ method. GAPDH is the housekeeping gene used for normalization in all qPCR assays. All primers used in this study and their respective sources or design are listed in Supplemental Material, Table S1.

SPP1 Western Blotting and ELISA

SPP1 levels were assessed in whole cell extract using standard Western blotting procedures with 1:1000 Anti-Osteopontin antibody (EPR3688, abcam). Relative protein concentrations were quantified in Image-J (NIH). SPP1 levels in cell culture media was assessed using the Human Osteopontin (OPN) Quantikine ELISA Kit (DOST00, R&D Systems). Media was sampled 60 hours post-transfection, after 48 hours of contact with the cells.

ChIP (Chromatin Immunoprecipitation) assay

NSCs were expanded to approximately 8 million cells, of which half were enriched for NRF2 using siRNA knockdown of NRF2's negative regulator KEAP1 and the other half were transfected with a non-targeting siRNA control. Samples were prepared following the SimpleChIP Plus Enzymatic Chromatin IP Kit protocol supplied by the manufacturer (Cell Signaling Technology). Briefly, 48 hours post transfection, NRF2 was cross-linked to DNA using 1.5% formaldehyde. Nuclei were collected and lysed by sonication. Chromatin DNA was

digested with Micrococcal Nuclease for 18 minutes into small fragments (150-900 bp). Nuclear extracts were incubated overnight with NRF2 antibody (cat. #12721, Cell Signaling Technology) and antibody-bound complexes were captured by protein G magnetic beads. Bound DNA was purified and underwent quantitation by PCR using primers for putative SPP1 ARE, NQO1 ARE (Chorley et al. 2012) and RPL30-exon 3 (Cell Signaling Technology).

The ELEMENT cohort, Pb exposure, and neurodevelopmental indexes

The cohort of infants analyzed in this study is a subset of the Early Life Exposures in Mexico and NeuroToxicology (ELEMENT) prospective birth cohort, which was designed to assess the roles of environmental and social stressors in birth outcomes as well as infant and child development. The characteristics of the cohort are provided in Supplemental Material, Table S2. Between 2007 and 2011, mothers were recruited during pregnancy and only one child for each mother was included in the study. Relevant to this study, prenatal Pb exposure was assessed from maternal blood during the second trimester of pregnancy. Infant neurodevelopment was assessed at 24 months of age using a Spanish version of the Bayley Scales of Infant and Toddler Development, Third Edition (Bayley 2005). Three primary outcome indices are derived from the assessment: the Cognitive Development Index (CDI), the Language Development Index (LDI) and the Psychomotor Development Index (PDI). Detailed information on the study design and data collection procedures have been published previously (Ettinger et al. 2009; Gonzalez-Cossio et al. 1997; Hernandez-Avila et al. 2002). The human subjects committees of the National Institutes of Public Health in Mexico, Harvard T.H. Chan School of Public Health, Icahn School of Medicine at Mt. Sinai, and participating hospitals approved all study materials and procedures.

Women and children old enough signed informed consent letters before enrollment. Consent obtained at enrollment applies to the research described in this study.

Prenatal Pb Exposure Assessed in Second Trimester Maternal Blood

In the second trimester of each expectant mother, maternal venous blood was collected in trace element-free tubes and frozen. Samples were shipped at 4°C to the Trace Metals Laboratory at the Harvard T.H. Chan School of Public Health, Boston, MA. Samples were processed in a dedicated trace metal clean room outfitted with a Class 100 clean hood using glassware cleaned for 24 hours in 10% HNO₃ and rinsed several times with 18Ω Milli-Q water. Approximately 1 g of blood from each mother was digested in 2 ml concentrated nitric acid for 24 hours, and subsequently overnight in 30% hydrogen peroxide (1 ml per 1 g of blood). Samples were diluted to 10 ml with deionized water. Acid-digested samples were analyzed for total Pb using dynamic reaction cell-inductively coupled plasma mass spectrometry (DRC-ICP-MS, Perkin Elmer). Final values are the average of five replicate measurements for each individual sample.

Assessment Using the Bayley Scales of Infant and Toddler Development

Infant neurodevelopment was assessed at 24 months of age using a Spanish version of the Bayley Scales of Infant and Toddler Development, Third Edition (Bayley 2005). Three primary outcome indices were derived from the assessment: the Cognitive Development Index (CDI), a composite variable of test scores pertaining to cognition; Language Development Index (LDI), a composite variable of test scores pertaining to expressive and receptive language; and the

Psychomotor Development Index (PDI) score, a composite variable of test scores pertaining to fine and gross motor skills.

Genome-wide Genotyping using an Illumina SNP Chip

DNA was extracted from umbilical cord blood samples in the ELEMENT cohort using the Puregene DNA isolation kit (Gentra Systems) and stored at -20°C. Samples were genotyped using the high density Illumina 1 Million Duo chip at the Center for Applied Genomics Core of the Children's Hospital of Philadelphia.

SNP analyses for main effect and Pb interaction

Following the quality control assessment, genotypes of 16 SNPs within the *SPP1* transcribed locus or within the 10 kilobase flanking regions were available for 462 infants in the ELEMENT cohort. Linear regression analyses for both main effect and interaction were performed using PLINK (Purcell et al. 2007). For main effect, linear regression analyses of minor allele copy number on the three outcomes (CDI, LDI and PDI) were adjusted for sex, gestational age, maternal age, marital status, presence of siblings, maternal education (high school vs no high school), age at Bayley Scale assessment and genome-wide principal components 1 and 2. For interaction analyses, natural log transformation of second trimester maternal blood Pb and a multiplicative interaction term of minor allele copy number and natural log transformation of second trimester maternal blood Pb were included in regression analyses. The p-value cut off for statistical significance was determined using the method proposed by (Li and Ji 2005), which takes into account that each SNP test is not an independent test given the

linkage disequilibrium (LD) among neighboring SNPs. A LD map and haplotypes were generated using the genotyped data using LDPlus (Vanderbilt University).

Results

RNA-seq identified gene expression changes in Pb-treated NSCs

To better understand the effects of Pb on NSCs, we performed global transcriptional profiling in human NSCs exposed to Pb. We chose to use RNA sequencing (RNA-seq) as we reasoned that the sensitivity of the method might allow for the identification of subtle yet significant changes in gene expression. Because we were particularly interested in the effect of Pb on prenatal neurodevelopment, we used human NSCs that were initially generated from an embryonic stem cell line (H09 line). We exposed cultured human NSCs to Pb or vehicle control (Fig. 1A). The Pb concentration used in this study (1 μ M, or 20.7 μ g/dl) is about four times of the current CDC level of concern for blood Pb and is within the range in exposed human populations (Pirkle et al. 1994; Zheng et al. 2008). Exposure of NSCs cells to 1 μ M Pb for 24 hours resulted in a slight decrease (5%) in cell number compared to that in the control vehicle-treated cells (Figure 1B). This is consistent with previous studies showing the inhibitory effect of Pb on NSC proliferation (Breier et al. 2008; Huang and Schneider 2004).

Using total RNAs from control and Pb-treated NSCs, we constructed RNA-seq libraries, each with a unique barcode that allows multiplexing. To minimize the variation of sequencing runs, we pooled barcoded RNA-seq libraries for Next-Gen sequencing. We obtained an average of ~38 million reads per sample and tested for differential expression of GRCh37 Ensembl-annotated genes. Following a stringent Benjamini-Hochberg multiple testing correction ($\alpha < 0.05$), we identified a total of 19 differentially expressed genes (3 down-regulated and 16 upregulated) in Pb-treated NSCs, as shown in Table 1 and in the volcano plot in Figure 1C. Full

results from the differential expression analysis are included in Supplementary Material, Excel File Table S1.

Effects of Pb on NRF2 target gene expression

Among the most statistically significant upregulated genes in Pb-treated NSCs are *NQO1* and *HMOX1*, which are well known classical targets involved in the cellular response to oxidative stress. The cellular oxidative stress response is mediated by the master transcriptional factor NRF2 (Kensler et al. 2007). NRF2 works to activate transcription by binding to the antioxidant responsive elements (AREs) in target genes. Many genes in addition to *NQO1* and *HMOX1* also contain ARE elements and are targets of NRF2. We thus examined the rest of the Pb-upregulated genes and found that at least 10 out of 16 genes had been previously identified as direct targets of NRF2 (Table 1). The expression changes of many of these genes induced by Pb were confirmed by qPCR. As shown in Fig. 1D, there is a remarkable consistency between the levels of gene expression measured by RNA-seq and qPCR. The induction of *NQO1*, *HMOX1* and the other known NRF2 target genes strongly suggests that Pb elicits oxidative stress and activates NRF2 in NSCs. Using *NQO1* expression as a surrogate marker for NRF2 activation, we determined the dose response of NSCs to Pb. As shown in Fig. 1E, Pb at as low as 0.1 μ M induced a significant increase (33%) in *NQO1* expression, indicating that NRF2 activation may be particularly sensitive to Pb exposure in NSCs.

Effect of Pb on SPP1 Expression

Four genes (SPP1, F2RL2, EGF and SLC7A8) that were not previously known as NRF2 targets are upregulated by Pb in NSCs (Figure 1C and Table 1). SPP1, also known as osteopontin

(OPN), is an extracellular matrix protein that has been shown to be upregulated in neuro-injury and is implicated as a potent neuroprotectant (Meller et al. 2005; Topkuru et al. 2013). Because of its potential connection to neural function, SPP1 was chosen for the follow up characterization. The upregulation of SPP1 by Pb in NSC cells was confirmed by qRT-PCR (Figure 2A). The *SPP1* gene has three splice variants, all of which were upregulated upon Pb exposure (Figure 2B), indicating that the mechanism involved in *SPP1* upregulation by Pb is not splicing variant-specific. Comparison of Ct values indicates SPP1-A is the dominant form in NSCs, with mRNA levels ~10-fold higher than SPP1-B and ~20-fold higher than SPP1-C (data not shown). Dose response showed that Pb induced SPP1 mRNA expression at 0.1 μ M and that the effect maximized at around 2 μ M (Figure 2C). The extent of SPP1 induction by Pb was higher at 20 hours than at later time points (Figure 2D), suggesting a potential negative feedback regulation of SPP1 mRNA expression. Consistent with mRNA upregulation, Western blotting showed that total SPP1 protein level is increased in Pb-treated NSCs (Figure 2E). Since SPP1 is a secreted protein, we measured the amount of SPP1 protein in the culture medium of Pb-exposed and unexposed NSCs. As shown in Figure 2F, there was more SPP1 protein in the media of NSCs cell culture of Pb-exposed NSCs than that in the control cells. After 60 hours of Pb exposure, the level of SPP1 in culture media of Pb-exposed cells was 1.8-fold higher than in unexposed cells.

Studies have shown that SPP1 is pro-proliferative (Kalluri and Dempsey 2012) and mediates the survival and proliferation of neural stem cells (Rabenstein et al. 2015). SPP1 upregulation by Pb thus may constitute a mechanism to protect NSCs from Pb toxicity. We have shown that Pb inhibits hNSC proliferation (Figure 1B). We thus determined whether SPP1 attenuates the inhibitory effect of Pb on hNSCs proliferation. As shown in Figure 2G, addition of

recombinant human SPP1 protein at 250 ng/ml in the culturing medium significantly increased the growth of hNSCs in the presence of Pb (90% vs. 79%). Even at lower concentration (50 ng/ml), SPP1 still increased hNSC cell growth in Pb-treated hNSCs, though to a lesser extent. These data support a neuroprotective role of SPP1 in reducing Pb toxicity in hNSCs.

The role of NRF2 in Pb-induced SPP1 upregulation

We next determined whether *SPP1* upregulation by Pb in NSCs is part of the NRF2-mediated oxidative stress response. We exposed NSCs to the canonical NRF2 activator DL-Sulforaphane. As shown in Figure 3A, 1 μ M DL-Sulforaphane significantly induced the expression of *NQO1* and *SPP1* expression. NRF2 is normally sequestered and degraded in the cytoplasm by its negative regulator KEAP1 (Kensler et al. 2007). Upon oxidative stress, NRF2 dissociates from KEAP1, accumulates and then translocates to the nucleus. Thus, NRF2 can be activated by inactivation of KEAP1. A pooled siRNA-mediated knocked down of KEAP1 by >70% (Figure 3B) led to an increase in both *SPP1* mRNA (9.6-fold 48 hours post siRNA transfection) and in the secreted SPP1 protein (3.9-fold, 60 hours post siRNA transfection) (Figure 3C and 3D). Together, these results indicate that NRF2 activation leads to increased *SPP1* expression.

To test whether NRF2 is required for *SPP1* upregulation, we knocked down NRF2 in NSCs and subsequently subjected the NSCs to Pb treatment. As shown in Figure 3E, two siRNAs both efficiently knocked down *NRF2*. Pb exposure itself did not affect either the baseline NRF2 expression or the knockdown efficiency (Figure 3E). However, knockdown of NRF2 significantly attenuates Pb-induced *SPP1* upregulation (Figure 3F). The effect is likely

specific as two different NRF2 siRNAs produced similar attenuation on *SPP1* upregulation. These data indicate that upregulation of *SPP1* by Pb exposure in NSCs is mediated by NRF2.

Direct transcriptional regulation of SPP1 by NRF2

NRF2 controls target gene expression by binding to specific DNA sequences known as Antioxidant Response Elements (AREs) within the promoters of target genes. Analyses of AREs in the promoters of canonical NRF2 target genes have identified a consensus sequence motif (RTKAYnnnGCR) that is required for NRF2 binding (Erickson et al. 2002). Using an ARE position weight matrix (Wang et al. 2007), we examined the promoter of *SPP1* and identified a putative ARE sequence ~600 base pairs upstream of the transcription start site (Figure 4A). To test whether NRF2 directly interacts with the putative *SPP1* ARE, we performed a ChIP (Chromatin Immuno-Precipitation) assay. We used KEAP1 knockdown to increase the NRF2 signal in NSCs. The NRF2 protein was immunoprecipitated and bound DNA fragments were examined to detect the presence of the putative *SPP1* ARE sequence. We compared the signal level in control and KEAP1-knockdown cells. As shown in Figure 4B, the qPCR signal specific to the *SPP1* ARE in KEAP1-knockdown NSCs was significantly higher than that in control NSCs. A similar increase was also observed for a canonical ARE located upstream of *NQO1*, whereas no significant increase was observed for a non-NRF2 target sequence, *RPL30-exon 3*. In addition, control ChIP using rabbit IgG showed very little pull down of *SPP1* ARE and there was no difference between KEAP1-knockdown and control cells (Supplementary Material Figure S1). Together these data indicate that *SPP1* gene contains a functional ARE and is a direct target of NRF2.

Association of SPP1 genetic polymorphism with cognitive development

Because NSCs play an important role in early brain development, we directly examined the association of SPP1 genetic variants with neurodevelopmental outcomes affected by Pb exposure in children. We took advantage of existing genotyping data from genome-wide association studies (GWAS) in the ELEMENT cohort (Wang et al., unpublished information), which was designed to assess the roles of environmental and social stressors in birth outcomes. A total of 16 common *SPP1* SNPs (minor allele frequency >5%) were genotyped in the ELEMENT cohort (n=462). The relative genomic location and linkage disequilibrium (LD) of the SNPs are shown in Fig. 5A. We performed regression analyses to examine the main effect of the SNPs on the three cognitive outcomes (Cognitive Development Index [CDI], Language Development Index [LDI], and Psychomotor Development Index [PDI]) as well as the SNP interaction with Pb exposure (Table 2). From these analyses, we identified the SNP rs12641001 with a statistically significant main effect association with CDI ($p=0.005$) (Fig. 5B). Rs12641001 does not show a statistically significant interaction with second trimester Pb exposure. According to the model each copy of the minor allele, T, increases CDI by 2.6 points. Upon examining the LD map (Fig. 5A), we found the T-allele of rs12641001 tags two haplotypes that spans the *SPP1* promoter region and the first part of the transcript. One of the tagging SNPs (rs2728127) is suggestively associated with CDI with raw p-value of 0.03471. Rs12641001 is suggestively associated with LDI ($p=0.078$), but has no evident association with PDI ($p=0.4089$). Therefore, rs12641001 has the largest and most significant association with CDI in children (Fig. 5B).

Discussion

In this study, we showed that Pb exposure induces an NRF2-mediated transcriptional response in neural stem cells. In particular we identified *SPP1* as a novel NRF2 target gene that is upregulated by Pb. We further demonstrated the association of a SPP1 genetic polymorphism with cognition development in children. By integrating the global transcriptomic profiling with genetic epidemiology, our study revealed SPP1 upregulation as a potential mechanistic link between Pb-induced gene expression in NSCs and neurodevelopment in children.

Our study is consistent with other reports of NRF2 activation and up-regulation of NRF2 targets by Pb (Korashy and El-Kadi 2006; Simmons et al. 2011; Yang et al. 2007; Zeller et al. 2010). We note, however, that some transcription profiling studies of Pb-exposed animals (Peterson et al. 2011; Schneider et al. 2012) have not identified NRF2 targets among the top hits. This could be due to the numerous secondary effects of Pb in animals undergoing long-term exposure, as these effects may crowd out the primary cellular transcriptional response. Furthermore, compensatory regulation of the NRF2 pathway may bring down the level of NRF2 activation upon long-term exposure. Although further study is needed to determine the exact mechanisms of Pb's activation of NRF2, our results implicate NRF2 activation as a new mechanism by which Pb affects NSCs function and neurodevelopment.

We identified *SPP1* as a Pb-induced gene and further demonstrated that *SPP1* is a novel NRF2 target. SPP1 is a pleiotropic extracellular glycoprotein with emerging roles in the brain as a potential neuroprotectant. SPP1 in the brain is upregulated in several morphological stress conditions including hypoxic ischemia (Albertsson et al. 2014; Chen et al. 2009; Meller et al. 2005), cortical lesion (Chan et al. 2014) and subarchnoid hemorrhage (Topkoku et al. 2013). SPP1 is also induced by a variety of environmental exposures, including cigarette smoke (Shan

et al. 2012) and ozone (Bass et al. 2013) in the lung, by chronic manganese exposure in the frontal cortex of manganese exposed non-human primates (Guilarte et al. 2008), and by ethanol in human primary neurospheres in culture (Vangipuram et al. 2008). As a secreted protein, SPP1 binds to and activates β 3-integrin (β 3) to initiate a Focal Adhesion Kinase (FAK) and Protein Kinase B (Akt)-dependent signaling. The β 3/FAK/Akt signaling axis is usually anti-apoptotic and pro-proliferative (Fong et al. 2009; Kalluri and Dempsey 2012; Meller et al. 2005; Topkora et al. 2013). Therefore, SPP1 upregulation by Pb and secretion from NSCs may induce a compensatory growth and survival response in NSCs and other neural cells.

While this is the first report indicating SPP1 is a direct target of NRF2, a relationship between the two factors has been suggested previously. Consistent with our finding that oxidative stress increases SPP1 expression, exposure of MG63 cells to the oxidative stress inhibitor n-acetylcysteine (NAC) down-regulates SPP1 expression (Kim et al. 2011). In addition, SPP1-mediated signaling through Akt and ERK is suggested to affect migration in glioma cells by activation of NRF2 (Lu et al. 2012), which would suggest a positive feedback loop. The regulatory feedback, however, is complicated by a possible negative feedback loop in which HMOX1, an NRF2 target, suppresses the transcription factor RUNX2, which positively regulates SPP1 expression (Kook et al. 2015). Further studies are needed to untangle the regulatory dynamics and to better understand their implications for Pb-mediated regulation of SPP1 in neurodevelopment.

The role of SPP1 in Pb neurotoxicity is further strengthened by the association of SPP1 variants with cognitive development in the ELEMENT birth cohort. Pb exposure has been repeatedly linked to neurocognitive dysfunction (Fulton et al. 1987; Hu et al. 2006; Needleman et al. 1979; Needleman et al. 1996; Wasserman et al. 1997). We identified a SNP, rs12641001,

with a statistically significant main effect association with CDI. A second SNP, rs2853744, had a near significant main effect association with LDI. The locations of rs12641001 and rs2853744 upstream of SPP1 suggest a possible role of these SNPs in the regulation of SPP1 gene expression. Despite our *in vitro* evidence for a neuroprotective role of SPP1 in Pb-treated hNSCs, we did not identify statistically significant interaction between any of the SPP1 SNPs and Pb exposure. Given that the sample size needed to detect significant gene and environment interactions is in general much larger than that for detecting main effects, it is likely that our ELEMENT cohort was underpowered to identify such interactions. Further epidemiological studies of a larger cohort are needed to test this and to help identify the causal variants in SPP1 that determine the neurodevelopment outcomes in children exposed to Pb.

Conclusions

The results we reported here reveal that Pb induces an NRF2-mediated transcriptional response, including the upregulation of a novel NRF2 target SPP1 in NSCs, and that SPP1 genetic polymorphism is associated with neurodevelopment outcomes in children. Our study thus identified SPP1 upregulation as a potential novel mechanism linking Pb exposure with neural stem cell function and neurodevelopment in children. Further mechanistic studies are needed to elucidate the role of SPP1 and NRF2 activation in modulating the effects of Pb on NSC function and neurodevelopment.

References

- Albertsson AM, Zhang X, Leavenworth J, Bi D, Nair S, Qiao L, et al. 2014. The effect of osteopontin and osteopontin-derived peptides on preterm brain injury. *J Neuroinflammation* 11:197.
- Alkondon M, Costa AC, Radhakrishnan V, Aronstam RS, Albuquerque EX. 1990. Selective blockade of nmda-activated channel currents may be implicated in learning deficits caused by lead. *FEBS Lett* 261:124-130.
- Bass V, Gordon CJ, Jarema KA, MacPhail RC, Cascio WE, Phillips PM, et al. 2013. Ozone induces glucose intolerance and systemic metabolic effects in young and aged brown norway rats. *Toxicol Appl Pharmacol* 273:551-560.
- Bayley N. 2005. Bayley scales of infant and toddler development. 3rd ed. San Antonio, TX:Pearson.
- Bellinger D, Leviton A, Waternaux C, Needleman H, Rabinowitz M. 1987. Longitudinal analyses of prenatal and postnatal lead exposure and early cognitive development. *New England Journal of Medicine* 316:1037-1043.
- Bellinger DC. 2013. Prenatal exposures to environmental chemicals and children's neurodevelopment: An update. *Safety and health at work* 4:1-11.
- Bellinger DC. 2016. Lead contamination in flint--an abject failure to protect public health. *The New England journal of medicine* 374:1101-1103.
- Breier JM, Radio NM, Mundy WR, Shafer TJ. 2008. Development of a high-throughput screening assay for chemical effects on proliferation and viability of immortalized human neural progenitor cells. *Toxicological Sciences* 105:119-133.
- Canfield RL, Henderson CR, Jr., Cory-Slechta DA, Cox C, Jusko TA, Lanphear BP. 2003. Intellectual impairment in children with blood lead concentrations below 10 microg per deciliter. *N Engl J Med* 348:1517-1526.
- Chan JL, Reeves TM, Phillips LL. 2014. Osteopontin expression in acute immune response mediates hippocampal synaptogenesis and adaptive outcome following cortical brain injury. *Exp Neurol* 261:757-771.
- Chen YJ, Wei YY, Chen HT, Fong YC, Hsu CJ, Tsai CH, et al. 2009. Osteopontin increases migration and mmp-9 up-regulation via alphavbeta3 integrin, fak, erk, and nf-kappab-dependent pathway in human chondrosarcoma cells. *J Cell Physiol* 221:98-108.

Cho HY, Reddy SP, Debiase A, Yamamoto M, Kleeberger SR. 2005. Gene expression profiling of nrf2-mediated protection against oxidative injury. *Free Radical Biology and Medicine* 38:325-343.

Chorley BN, Campbell MR, Wang X, Karaca M, Sambandan D, Bangura F, et al. 2012. Identification of novel nrf2-regulated genes by chip-seq: Influence on retinoid x receptor alpha. *Nucleic Acids Res* 40:7416-7429.

Erickson AM, Nevarea Z, Gipp JJ, Mulcahy RT. 2002. Identification of a variant antioxidant response element in the promoter of the human glutamate-cysteine ligase modifier subunit gene. Revision of the are consensus sequence. *J Biol Chem* 277:30730-30737.

Ettinger AS, Lamadrid-Figueroa H, Tellez-Rojo MM, Mercado-Garcia A, Peterson KE, Schwartz J, et al. 2009. Effect of calcium supplementation on blood lead levels in pregnancy: A randomized placebo-controlled trial. *Environ Health Perspect* 117:26-31.

Fong YC, Liu SC, Huang CY, Li TM, Hsu SF, Kao ST, et al. 2009. Osteopontin increases lung cancer cells migration via activation of the alphavbeta3 integrin/fak/akt and nf-kappab-dependent pathway. *Lung Cancer* 64:263-270.

Fulton M, Raab G, Thomson G, Laxen D, Hunter R, Hepburn W. 1987. Influence of blood lead on the ability and attainment of children in edinburgh. *Lancet* 1:1221-1226.

Gibbs RA. 2003. The international hapmap project. *Nature* 426:789-796.

Gilbert ME, Kelly ME, Samsam TE, Goodman JH. 2005. Chronic developmental lead exposure reduces neurogenesis in adult rat hippocampus but does not impair spatial learning. *Toxicological Sciences* 86:365-374.

Gonzalez-Cossio T, Peterson KE, Sanin LH, Fishbein E, Palazuelos E, Aro A, et al. 1997. Decrease in birth weight in relation to maternal bone-lead burden. *Pediatrics* 100:856-862.

Guilarte TR, Miceli RC. 1992. Age-dependent effects of lead on [3h]mk-801 binding to the nmda receptor-gated ionophore: In vitro and in vivo studies. *Neurosci Lett* 148:27-30.

Guilarte TR, Burton NC, Verina T, Prabhu VV, Becker KG, Syversen T, et al. 2008. Increased ap1 expression and neurodegeneration in the frontal cortex of manganese-exposed non-human primates. *Journal of Neurochemistry* 105:1948-1959.

Hernandez-Avila M, Peterson KE, Gonzalez-Cossio T, Sanin LH, Aro A, Schnaas L, et al. 2002. Effect of maternal bone lead on length and head circumference of newborns and 1-month-old infants. *Arch Environ Health* 57:482-488.

Hu H, Tellez-Rojo MM, Bellinger D, Smith D, Ettinger AS, Lamadrid-Figueroa H, et al. 2006. Fetal lead exposure at each stage of pregnancy as a predictor of infant mental development. *Environmental health perspectives* 114:1730-1735.

- Huang F, Schneider JS. 2004. Effects of lead exposure on proliferation and differentiation of neural stem cells derived from different regions of embryonic rat brain. *Neurotoxicology* 25:1001-1012.
- Jones RL, Homa DM, Meyer PA, Brody DJ, Caldwell KL, Pirkle JL, et al. 2009. Trends in blood lead levels and blood lead testing among us children aged 1 to 5 years, 1988-2004. *Pediatrics* 123:e376-385.
- Kalluri HS, Dempsey RJ. 2012. Osteopontin increases the proliferation of neural progenitor cells. *Int J Dev Neurosci* 30:359-362.
- Kensler TW, Wakabayashi N, Biswal S. 2007. Cell survival responses to environmental stresses via the keap1-nrf2-are pathway. *Annu Rev Pharmacol Toxicol* 47:89-116.
- Kim NR, Lim BS, Park HC, Son KM, Yang HC. 2011. Effects of n-acetylcysteine on tegdma- and hema-induced suppression of osteogenic differentiation of human osteosarcoma mg63 cells. *J Biomed Mater Res B Appl Biomater* 98:300-307.
- Kook SH, Kim KA, Ji H, Lee D, Lee JC. 2015. Irradiation inhibits the maturation and mineralization of osteoblasts via the activation of nrf2/ho-1 pathway. *Mol Cell Biochem* 410:255-266.
- Korashy HM, El-Kadi AO. 2006. Transcriptional regulation of the nad(p)h:Quinone oxidoreductase 1 and glutathione s-transferase ya genes by mercury, lead, and copper. *Drug Metab Dispos* 34:152-165.
- Lee JM, Calkins MJ, Chan K, Kan YW, Johnson JA. 2003. Identification of the nf-e2-related factor-2-dependent genes conferring protection against oxidative stress in primary cortical astrocytes using oligonucleotide microarray analysis. *Journal of Biological Chemistry* 278:12029-12038.
- Levin ED. 2016. Crumbling infrastructure and learning impairment: A call for responsibility. *Environmental health perspectives* 124:A79.
- Li J, Lee JM, Johnson JA. 2002. Microarray analysis reveals an antioxidant responsive element-driven gene set involved in conferring protection from an oxidative stress-induced apoptosis in imr-32 cells. *Journal of Biological Chemistry* 277:388-394.
- Li J, Ji L. 2005. Adjusting multiple testing in multilocus analyses using the eigenvalues of a correlation matrix. *Heredity (Edinb)* 95:221-227.
- Lu DY, Yeh WL, Huang SM, Tang CH, Lin HY, Chou SJ. 2012. Osteopontin increases heme oxygenase-1 expression and subsequently induces cell migration and invasion in glioma cells. *Neuro Oncol* 14:1367-1378.

- Malhotra D, Portales-Casamar E, Singh A, Srivastava S, Arenillas D, Happel C, et al. 2010. Global mapping of binding sites for nrf2 identifies novel targets in cell survival response through chip-seq profiling and network analysis. *Nucleic Acids Res* 38:5718-5734.
- Martin M. 2011. Cutadapt removes adapter sequences from high-throughput sequencing reads. *EMBnet* 17:10-12.
- Meller R, Stevens SL, Minami M, Cameron JA, King S, Rosenzweig H, et al. 2005. Neuroprotection by osteopontin in stroke. *J Cereb Blood Flow Metab* 25:217-225.
- Neal AP, Stansfield KH, Worley PF, Thompson RE, Guilarte TR. 2010. Lead exposure during synaptogenesis alters vesicular proteins and impairs vesicular release: Potential role of nmda receptor-dependent bdnf signaling. *Toxicological Sciences* 116:249-263.
- Neal AP, Worley PF, Guilarte TR. 2011. Lead exposure during synaptogenesis alters nmda receptor targeting via nmda receptor inhibition. *Neurotoxicology* 32:281-289.
- Needleman HL, Gunnoe C, Leviton A, Reed R, Peresie H, Maher C, et al. 1979. Deficits in psychologic and classroom performance of children with elevated dentine lead levels. *N Engl J Med* 300:689-695.
- Needleman HL, Riess JA, Tobin MJ, Biesecker GE, Greenhouse JB. 1996. Bone lead levels and delinquent behavior. *JAMA* 275:363-369.
- Opler MG, Brown AS, Graziano J, Desai M, Zheng W, Schaefer C, et al. 2004. Prenatal lead exposure, delta-aminolevulinic acid, and schizophrenia. *Environmental health perspectives* 112:548-552.
- Opler MG, Buka SL, Groeger J, McKeague I, Wei C, Factor-Litvak P, et al. 2008. Prenatal exposure to lead, delta-aminolevulinic acid, and schizophrenia: Further evidence. *Environmental health perspectives* 116:1586-1590.
- Peterson SM, Zhang J, Weber G, Freeman JL. 2011. Global gene expression analysis reveals dynamic and developmental stage-dependent enrichment of lead-induced neurological gene alterations. *Environmental health perspectives* 119:615-621.
- Pirkle JL, Brody DJ, Gunter EW, Kramer RA, Paschal DC, Flegal KM, et al. 1994. The decline in blood lead levels in the united states. The national health and nutrition examination surveys (nhanes). *JAMA* 272:284-291.
- Purcell S, Neale B, Todd-Brown K, Thomas L, Ferreira MA, Bender D, et al. 2007. Plink: A tool set for whole-genome association and population-based linkage analyses. *American journal of human genetics* 81:559-575.

- Rabenstein M, Hucklenbroich J, Willuweit A, Ladwig A, Fink GR, Schroeter M, et al. 2015. Osteopontin mediates survival, proliferation and migration of neural stem cells through the chemokine receptor cxcr4. *Stem cell research & therapy* 6:99.
- Robinson MD, Oshlack A. 2010. A scaling normalization method for differential expression analysis of rna-seq data. *Genome Biol* 11:R25.
- Sanchez-Martin FJ, Fan Y, Lindquist DM, Xia Y, Puga A. 2013. Lead induces similar gene expression changes in brains of gestationally exposed adult mice and in neurons differentiated from mouse embryonic stem cells. *PloS one* 8:e80558.
- Schneider JS, Anderson DW, Wade TV, Smith MG, Leibbrandt P, Zuck L, et al. 2005. Inhibition of progenitor cell proliferation in the dentate gyrus of rats following post-weaning lead exposure. *Neurotoxicology* 26:141-145.
- Schneider JS, Anderson DW, Talsania K, Mettil W, Vadigepalli R. 2012. Effects of developmental lead exposure on the hippocampal transcriptome: Influences of sex, developmental period, and lead exposure level. *Toxicological Sciences* 129:108-125.
- Senut MC, Sen A, Cingolani P, Shaik A, Land SJ, Ruden DM. 2014. Lead exposure disrupts global DNA methylation in human embryonic stem cells and alters their neuronal differentiation. *Toxicol Sci* 139:142-161.
- Shan M, Yuan X, Song LZ, Roberts L, Zarinkamar N, Seryshev A, et al. 2012. Cigarette smoke induction of osteopontin (spp1) mediates t(h)17 inflammation in human and experimental emphysema. *Sci Transl Med* 4:117ra119.
- Simmons SO, Fan CY, Yeoman K, Wakefield J, Ramabhadran R. 2011. Nrf2 oxidative stress induced by heavy metals is cell type dependent. *Curr Chem Genomics* 5:1-12.
- Stansfield KH, Pilsner JR, Lu Q, Wright RO, Guilarte TR. 2012. Dysregulation of bdnf-trkb signaling in developing hippocampal neurons by pb2+: Implications for an environmental basis of neurodevelopmental disorders. *Toxicological Sciences*.
- Thai P, Statt S, Chen CH, Liang E, Campbell C, Wu R. 2013. Characterization of a novel long noncoding rna, scal1, induced by cigarette smoke and elevated in lung cancer cell lines. *American Journal of Respiratory Cell and Molecular Biology* 49:204-211.
- Topkuru BC, Altay O, Duris K, Krafft PR, Yan J, Zhang JH. 2013. Nasal administration of recombinant osteopontin attenuates early brain injury after subarachnoid hemorrhage. *Stroke* 44:3189-3194.
- Toscano CD, Guilarte TR. 2005. Lead neurotoxicity: From exposure to molecular effects. *Brain Research Reviews* 49:529-554.

Trapnell C, Pachter L, Salzberg SL. 2009. Tophat: Discovering splice junctions with rna-seq. *Bioinformatics* 25:1105-1111.

Vangipuram SD, Grever WE, Parker GC, Lyman WD. 2008. Ethanol increases fetal human neurosphere size and alters adhesion molecule gene expression. *Alcohol Clin Exp Res* 32:339-347.

Verina T, Rohde CA, Guilarte TR. 2007. Environmental lead exposure during early life alters granule cell neurogenesis and morphology in the hippocampus of young adult rats. *Neuroscience* 145:1037-1047.

Wang X, Tomso DJ, Chorley BN, Cho HY, Cheung VG, Kleeberger SR, et al. 2007. Identification of polymorphic antioxidant response elements in the human genome. *Human Molecular Genetics* 16:1188-1200.

Wasserman GA, Liu X, Lolocono NJ, Factor-Litvak P, Kline JK, Popovac D, et al. 1997. Lead exposure and intelligence in 7-year-old children: The yugoslavia prospective study. *Environ Health Perspect* 105:956-962.

Yang L, Kemadjou JR, Zinsmeister C, Bauer M, Legradi J, Muller F, et al. 2007. Transcriptional profiling reveals barcode-like toxicogenomic responses in the zebrafish embryo. *Genome Biol* 8:R227.

Zeller I, Knoflach M, Seubert A, Kreutmayer SB, Stelzmuller ME, Wallnoefer E, et al. 2010. Lead contributes to arterial intimal hyperplasia through nuclear factor erythroid 2-related factor-mediated endothelial interleukin 8 synthesis and subsequent invasion of smooth muscle cells. *Arterioscler Thromb Vasc Biol* 30:1733-1740.

Zheng L, Wu K, Li Y, Qi Z, Han D, Zhang B, et al. 2008. Blood lead and cadmium levels and relevant factors among children from an e-waste recycling town in china. *Environmental Research* 108:15-20.

Table 1: Differential expression of human NSCs exposed to 1 μ M Pb by RNA-seq.

HGNC Name	Gene Description	Fold Change	p-value	FDR q-value	NRF2 Target
F2RL2	<i>coagulation factor II (thrombin) receptor-like 2</i>	2.35	1.05×10^{-19}	4.62×10^{-16}	
OSGIN1	<i>oxidative stress induced growth inhibitor 1</i>	2.29	8.21×10^{-12}	2.06×10^{-8}	a
LUCAT1	<i>lung cancer associated transcript 1 (non-protein coding)</i>	1.98	6.60×10^{-8}	1.16×10^{-4}	g
HMOX1	<i>heme oxygenase (decycling) 1</i>	1.87	4.63×10^{-15}	1.63×10^{-11}	a,b,d,e
SPP1	<i>secreted phosphoprotein 1</i>	1.82	3.27×10^{-22}	1.92×10^{-18}	
NQO1	<i>NAD(P)H dehydrogenase, quinone 1</i>	1.8	2.24×10^{-33}	3.93×10^{-29}	a,b,c,f
EGF	<i>epidermal growth factor</i>	1.45	4.07×10^{-7}	6.50×10^{-4}	
FTL	<i>ferritin, light polypeptide</i>	1.43	5.00×10^{-29}	4.39×10^{-25}	a,b
VGF	<i>VGF nerve growth factor inducible</i>	1.39	8.65×10^{-13}	2.53×10^{-9}	b
TXNRD1	<i>thioredoxin reductase 1</i>	1.38	1.22×10^{-9}	2.68×10^{-6}	a,b,f
SERPINE1	<i>serpin peptidase inhibitor, clade E (nexin, plasminogen activator inhibitor type 1), member 1</i>	1.36	1.53×10^{-6}	1.92×10^{-3}	b,c,f
SLC7A11	<i>solute carrier family 7 (anionic amino acid transporter light chain, xc- system), member 11</i>	1.34	1.20×10^{-5}	1.11×10^{-2}	a
SLC7A8	<i>solute carrier family 7 (amino acid transporter light chain, L system), member 8</i>	1.31	6.88×10^{-7}	1.01×10^{-3}	
GREM1	<i>gremlin 1, DAN family BMP antagonist</i>	1.28	5.19×10^{-6}	5.07×10^{-3}	
PIR	<i>pirin (iron-binding nuclear protein)</i>	1.25	8.54×10^{-7}	1.15×10^{-3}	a
F13A1	<i>coagulation factor XIII, A1 polypeptide</i>	1.24	5.05×10^{-5}	3.55×10^{-2}	
B3GALT2	<i>UDP-Gal:betaGlcNAc beta 1,3-galactosyltransferase, polypeptide 2</i>	0.81	3.00×10^{-5}	2.29×10^{-2}	
MIR503HG	<i>MIR503 host gene (non-protein coding)</i>	0.73	2.14×10^{-5}	1.79×10^{-2}	
DIO3OS	<i>DIO3 opposite strand/antisense RNA</i>	0.68	3.35×10^{-6}	3.47×10^{-3}	

Differential expression of triplicate pairs was performed in edgeR, and statistically significantly differentially expressed transcripts were defined by greater than $\pm 0.2 \log_2$ fold change and FDR-adjusted q-value $< 0.05\%$. Annotation shows known NRF2 target genes according to: a. (Chorley et al. 2012), b. (Wang et al. 2007), c. (Cho et al. 2005), d. (Lee et al. 2003), e. (Li et al. 2002), f. (Malhotra et al. 2010) and g. (Thai et al. 2013).

Table 2: Summary of SPP1 SNP association effect sizes and p-values in determining CDI, LDI and PDI.

rs id chr4 bpAllelesMAF				Cognitive Development Index (CDI)						Language Development Index (LDI)						Psychomotor Development Index (PDI)											
				Main Effect		Interaction				Main Effect		Interaction				Main Effect		Interaction									
				β	p-val	SNP β	SNP*logPb p-val	β	p-val	β	p-val	SNP β	SNP*logPb p-val	β	p-val	SNP β	SNP*logPb p-val	β	p-val	SNP β	SNP*logPb p-val						
rs4693923	88888113	A / G	0.11	-0.18	0.8338	-	0.65	0.6881	0.12	0.7425	0.44	0.6344	-	1.16	0.5047	0.45	0.2516	-0.77	0.4461	-3.96	0.03735	0.91	0.03547				
rs1264100188888940	T / C	0.10	2.56	0.00508	3.97	0.01465	-0.37	0.2723	1.72	0.078	2.44	0.1589	-0.22	0.5449	0.88	0.4089	3.82	0.04506	-0.65	0.1012							
rs6833161	88889605	T / C	0.32	0.26	0.6557	0.57	0.6011	-0.09	0.7115	0.58	0.3557	0.30	0.7952	0.07	0.7677	0.54	0.4271	0.28	0.8252	0.12	0.6611						
rs6813526	88894235	C / T	0.13	1.67	0.04771	2.67	0.06719	-0.24	0.3895	1.91	0.0324	1.89	0.2224	-0.01	0.9617	0.70	0.4694	3.20	0.06073	-0.54	0.1052						
rs2728127	88895115	G / A	0.14	1.69	0.03471	2.99	0.03169	-0.29	0.2822	1.93	0.02355	1.93	0.1899	-0.01	0.983	1.28	0.1667	3.68	0.02321	-0.49	0.1255						
rs2853744	88896248	T / G	0.07	1.64	0.1167	2.26	0.2209	-0.20	0.5934	3.01	0.00671	4.19	0.03141	-0.35	0.3725	1.34	0.2693	4.95	0.02173	-0.76	0.07875						
rs1173058288896421	T / C	0.46	0.53	0.3454	0.64	0.5377	-0.06	0.8091	0.97	0.1054	0.74	0.5008	0.04	0.8628	0.11	0.8629	-0.66	0.5887	0.24	0.3948							
rs1172869788898941	C / T	0.44	0.24	0.667	0.84	0.4201	-0.18	0.4622	0.92	0.1239	0.94	0.3916	0.00	0.996	0.09	0.8852	-0.14	0.9079	0.12	0.6655							
rs6811536	88902405	T / C	0.18	-0.49	0.4734	-	1.26	0.303	0.18	0.4957	-1.22	0.09704	-	1.38	0.2897	0.08	0.7932	-0.80	0.3165	0.31	0.8282	-0.33	0.2974				
rs4754	88902692	C / T	0.43	0.70	0.1951	0.23	0.8117	0.15	0.4827	0.92	0.1085	0.83	0.415	0.01	0.9576	0.84	0.1788	1.12	0.3191	-0.05	0.8477						
rs1126616	88903853	T / C	0.43	0.71	0.1878	0.28	0.7698	0.14	0.5191	0.87	0.1253	0.86	0.3963	-0.01	0.9741	0.81	0.1902	1.16	0.2997	-0.07	0.7927						
rs1126772	88904186	G / A	0.17	0.69	0.3339	2.29	0.1085	-0.41	0.229	0.90	0.237	0.85	0.5708	0.03	0.9273	0.53	0.5197	0.26	0.8748	0.12	0.7667						
rs9138	88904342	C / A	0.43	0.82	0.132	0.26	0.7909	0.18	0.4079	1.00	0.0842	0.84	0.4128	0.03	0.8925	0.85	0.1777	1.08	0.3378	-0.04	0.8841						
rs1001215088905795	C / T	0.17	0.63	0.37	2.16	0.1273	-0.39	0.245	0.88	0.234	0.71	0.6338	0.06	0.8647	0.74	0.3566	0.43	0.7946	0.13	0.7494							
rs7685225	88906458	C / T	0.11	0.83	0.3564	3.40	0.03468	-0.66	0.04885	0.12	0.8967	-	0.05	0.9769	0.01	0.9745	0.09	0.9341	1.02	0.5889	-0.30	0.4512					
rs7675246	88908998	A / G	0.18	-0.72	0.2987	-	1.60	0.1913	0.22	0.4219	-1.53	0.03807	-	1.97	0.1274	0.15	0.6057	-0.62	0.4351	0.67	0.6378	-0.38	0.2261				

Models were adjusted for sex, gestational age, maternal age, marital status, presence of siblings, maternal education, genome-wide principle components 1 and 2, and natural log of second trimester maternal blood Pb level. Alleles are written in the format minor allele / major allele.

According to the method proposed by (Li and Ji 2005), the p-value cut off for this analysis of SNPs in LD to maintain a 5% Type 1 error rate is 0.00568; a single significant result is marked with bold text. Main effects from interaction analysis are provided in Table S2 in Supplementary Information, Part 1.

Figure Legends

Figure 1: Identification of differential gene expression in human NSCs exposed to Pb by RNA-seq. (A) Schematic workflow of the study. (B) MTT assay showing relative numbers of NSCs after 24 hour treatment of Pb at different concentrations. Error bars represent standard error of the mean of 8 replicates. (C) Volcano plot of RNA-seq results with top 4 genes annotated. Black squares represent differentially expressed genes defined by greater than 0.2 log₂ fold change and FDR-adjusted q-value < 0.05%; gray circles represent genes that do not meet the significance threshold. (D) qPCR validation of known NRF2 targets identified by RNA-seq. Results were obtained from three biologic replicates. (E) Induction of *NQO1* expression in response to 24 hours Pb treatment (at different concentrations) in NSCs.

Figure 2: Effects of Pb treatment on SPP1 expression in NSCs. (A) Comparison of *SPP1* induction fold changes measured by qPCR and RNA-seq. (B) qPCR of three major *SPP1* splice variants after 24 hours Pb exposure. Splice-variant specific primers were used. (C) Dose-response curve of SPP1 exposed to a range of Pb concentrations for 24 hours. (D) Time course of SPP1 exposed to 1 μ M Pb. (E) Upper panel: SPP1 Western Blotting of whole cell extracts from control or 24-hour Pb-treated NSCs. Lower panel: relative SPP1 protein amount normalized against β -actin. (F) Cell culture media concentration of SPP1 determined by ELISA in control or Pb-treated NSCs (for 20, 40 and 60 hours). All error bars represent the standard error of the mean of three biologic replicates. (G) hNSCs seeded in 24 well plates at 5×10^4 per well were treated with control vehicle PBS or human recombinant SPP1 protein (Eton Bioscience) at 50 or 250 ng/ml. The next day, hNSCs were exposed to 2 μ M Pb for 3 days. Cell counting was done

by hemocytometer with Trypan blue staining to exclude dead cells. Six replicates were done for each condition.

Figure 3: NRF2-dependent upregulation of SPP1 expression . (A) *SPP1* and *NQO1* expression fold changes (measure by qPCR) in NSCs exposed to canonical NRF2 inducer DL-Sulforaphane (DLS, 1 μ M) for 24 hours. (B) Efficiency of siRNA knockdown of KEAP1 48 hours post transfection as assessed by qPCR. NT: non-targeting control siRNAs. (C) *SPP1* expression in control or KEAP1 knockdown NSCs. qPCR was done 48 hours post KEAP1 siRNA transfection. (D) Amount of secreted SPP1 protein in cultured media of NSCs at 60 hours post KEAP1 siRNA transfection. (E) Efficiency of siRNA knockdown of NRF2 using two siRNAs 48 hours post transfection. Pb and vehicle control were added to cells 24 hours post transfection for a 24-hour exposure. (F) SPP1 expression after 24 hours of Pb exposure in NRF2-knockdown cells compared to that in NT-siRNA transfected cells. All figure error bars represent standard error of the mean of three biologic replicates.

Figure 4: NRF2 interaction with an ARE in the SPP1 promoter. (A) Presence of a putative ARE ~600 bp upstream of SPP1 transcription start site. (B) NRF2 ChIP followed by PCR amplification of the putative SPP1 ARE. NRF2 was activated by KEAP1 knockdown and NT-siRNA was transfected into control cells. Following NRF2 ChIP, qPCR was done to measure the presence of SPP1 ARE, NQO1 ARE (positive control) and RPL30 Exon 3 (negative control).
*: $p < 0.05$ by two-sided t-test.

Figure 5: Association analysis of SPP1 SNPs with neurodevelopment phenotypes. (A) Schema of SNPs in relation to the *SPP1* transcribed locus and ARE. Linkage disequilibrium (LD) patterns around *SPP1* in the study population are shown. The relative abundances of haplotypes are shown above the LD plot. LD plot reflects pairwise R^2 among SNPs. (B) Negative log₁₀ p-values for SNP associations with the Cognitive Development Index (CDI), Language Development Index (LDI) and Psychomotor Development Index (PDI) as a main effect (G) and in interaction with maternal 2nd trimester lead (GxE).

Figure 1.

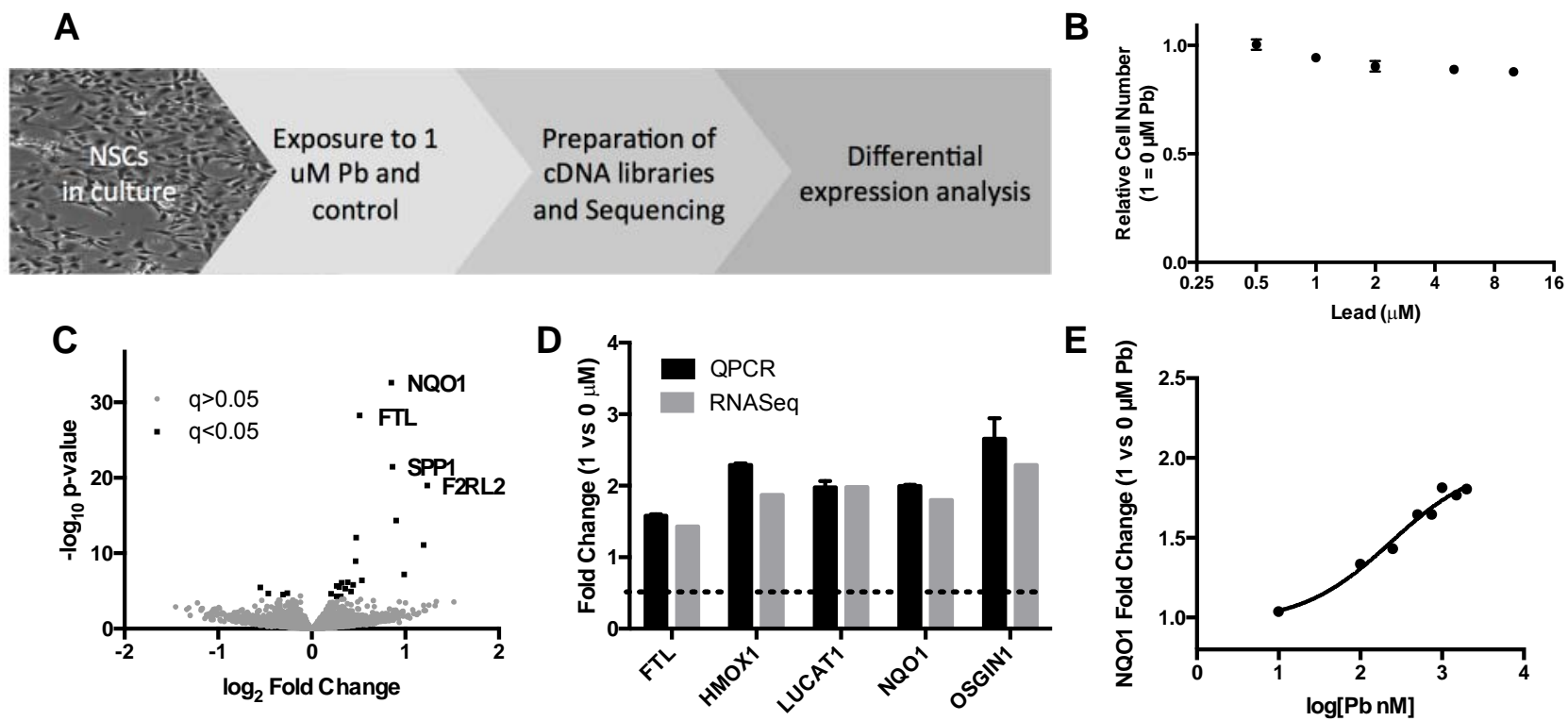


Figure 2.

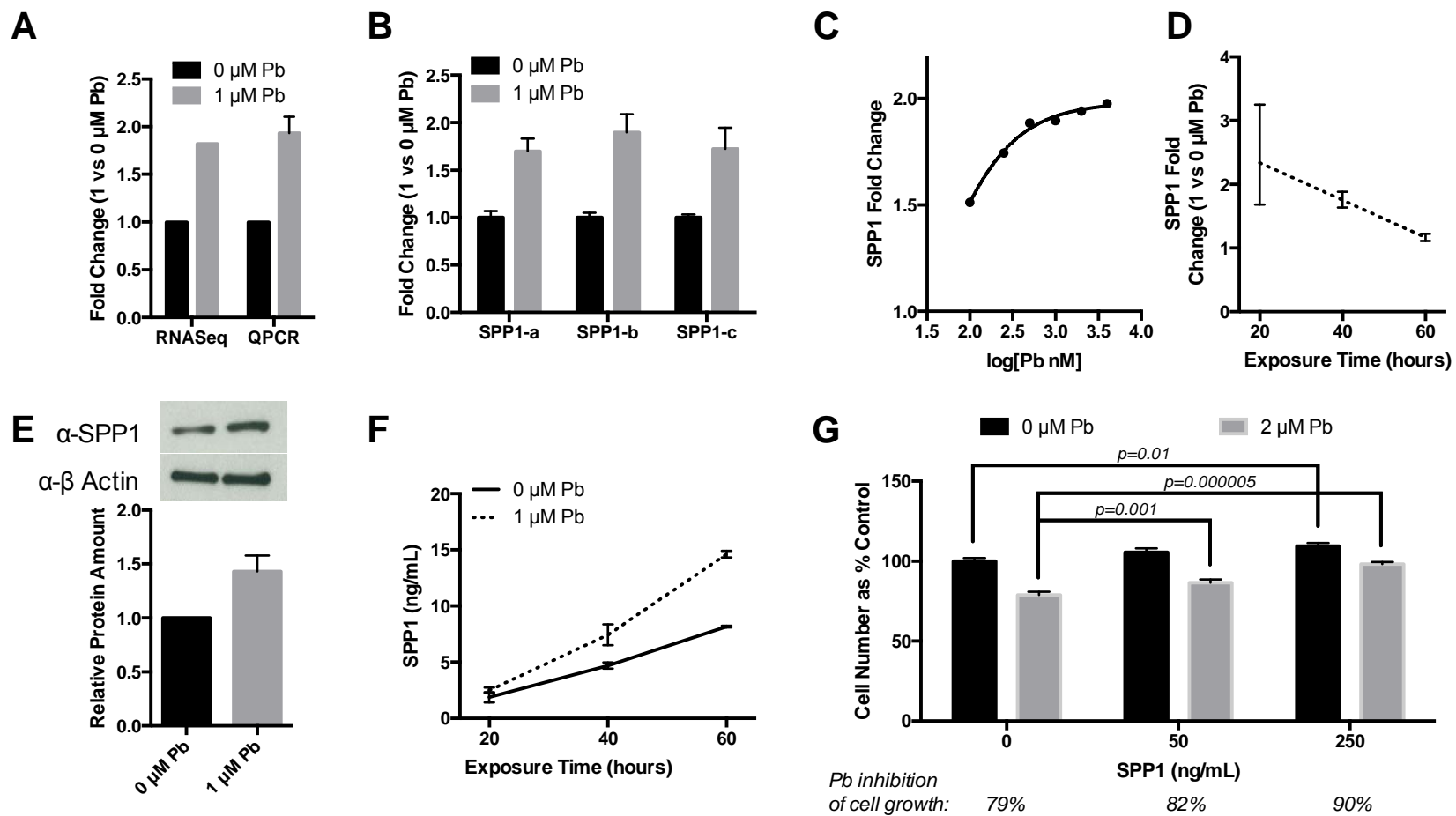


Figure 3.

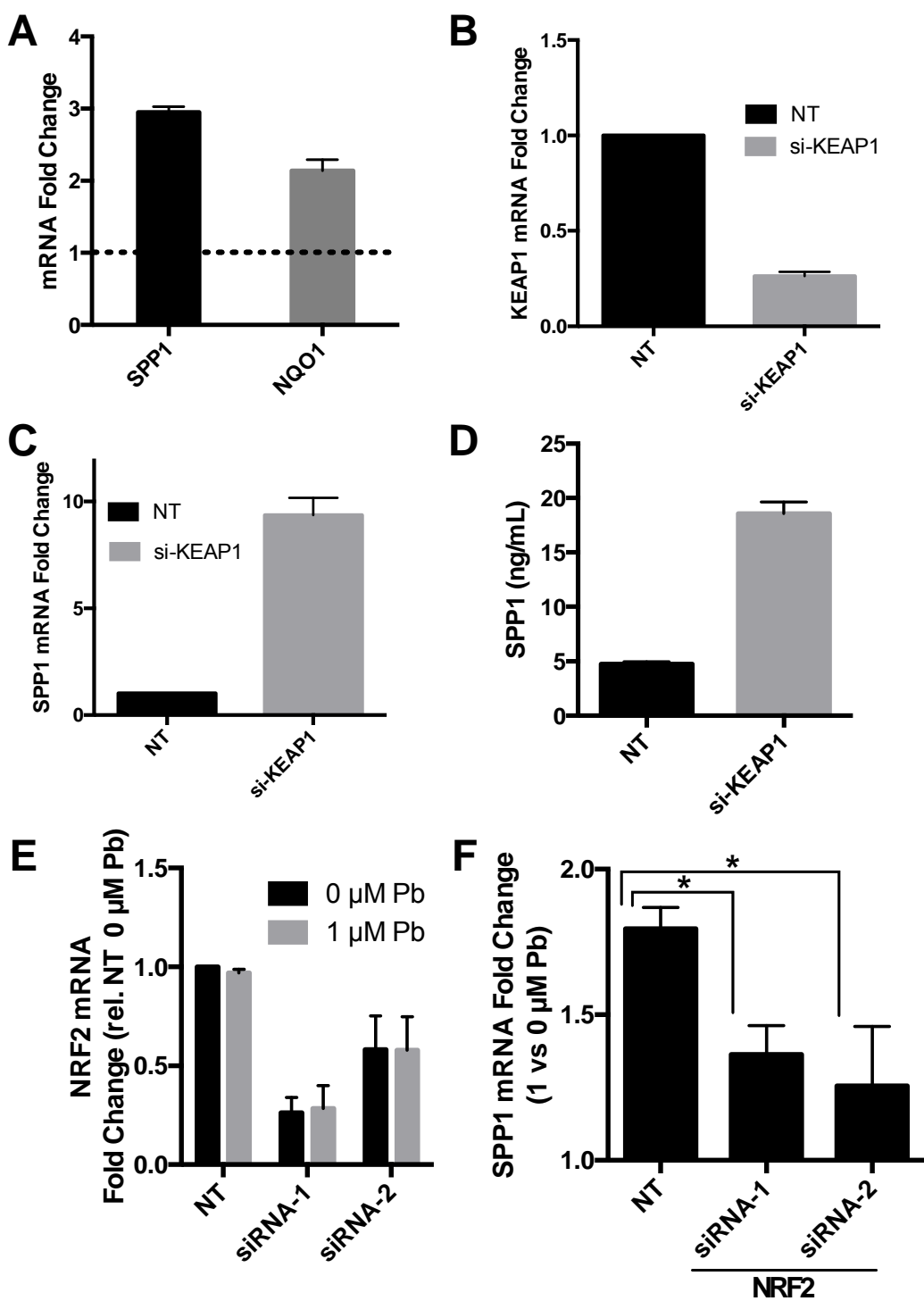


Figure 4.

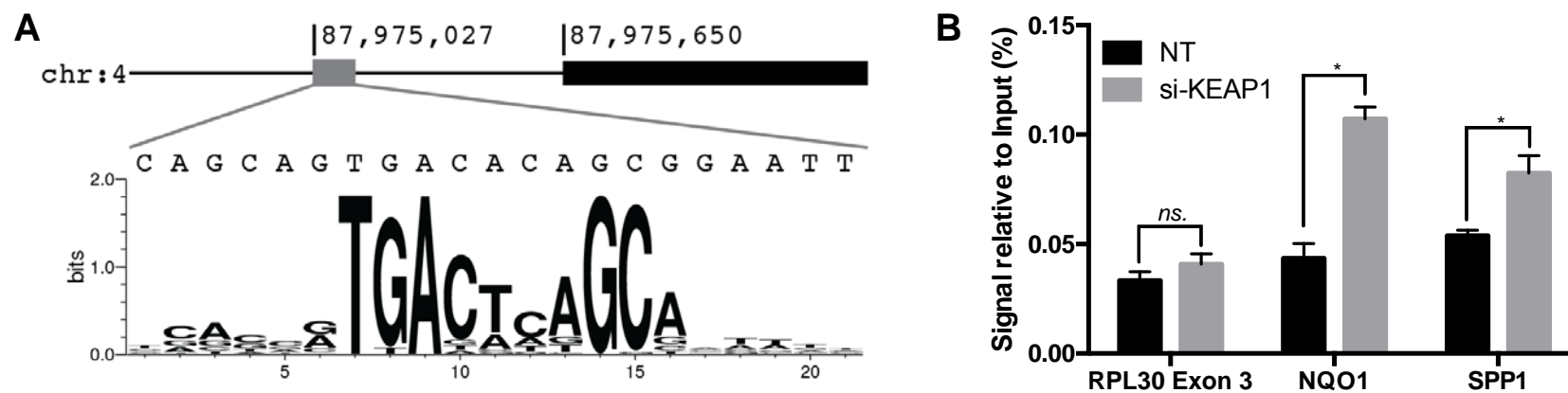


Figure 5.

